

Critical behaviour of two Ising models with near-neighbour exclusion

This article has been downloaded from IOPscience. Please scroll down to see the full text article.

1992 J. Phys. A: Math. Gen. 25 6231

(<http://iopscience.iop.org/0305-4470/25/23/019>)

View [the table of contents for this issue](#), or go to the [journal homepage](#) for more

Download details:

IP Address: 171.66.16.59

The article was downloaded on 01/06/2010 at 17:39

Please note that [terms and conditions apply](#).

Critical behaviour of two Ising models with near-neighbour exclusion

F Iglóit†, J R Heringa§, M M F Philippens§, A Hoogland§ and H W J Blöte§

† Laboratoire de Physique du Solide, URA CNRS 155, Université de Nancy I, F-54506 Nancy, France

§ Laboratorium voor Technische Natuurkunde, Postbus 5046, 2600 GA Delft, The Netherlands

Received 22 January 1992, in final form 28 May 1992

Abstract. We have performed extensive Monte Carlo simulations of two-dimensional layered Ising lattice gases with $(m - 1)$ -neighbour exclusion in the x direction and pair attraction in the y direction. We studied the specific heat of the models in systems with different rectangular shapes and the spin-spin correlation function in the x direction near to the critical point. For the $m = 3$ model both the thermal and magnetic exponents were estimated to be close to the known values of the three-state Potts model. Estimates for the critical exponents of the $m = 4$ model are consistent with a commensurate-incommensurate transition; however we find no independent evidence for the existence of a floating phase.

1. Introduction

We consider a two-dimensional anisotropic Ising lattice gas with ferromagnetic pair interaction in the y direction and with $(m - 1)$ -neighbour exclusion in the x direction. The reduced Hamiltonian of the model is

$$\mathcal{H} = \sum_{x,y} \left[K^y S_{x,y} S_{x,y+1} + K_1 S_{x,y} + \sum_{j=1}^{m-1} K_j^x (S_{x,y} + 1)(S_{x+j,y} + 1) \right] \quad (1.1)$$

i.e. \mathcal{H} and the couplings denoted by K contain a factor $-1/kT$. The spin variables take the values $S_{x,y} = \pm 1$, and $K_j^x = -\infty$ for $j = 1, 2, \dots, m - 1$ imposes the neighbour exclusion. Since two up-spins have to be at least a distance m apart, a hard rod with length m can be assigned to each plus spin. Thus (1.1) can be considered to describe the ordering phenomena of attractive hard rods in two dimensions. The low-temperature phase of (1.1) is m -fold degenerate. The phase coexistence is believed to end at a transition point. In this paper we verify this and investigate the properties of this phase transition for $m = 3$ and 4 for the case $K_1 = K_y$.

The model in (1.1) belongs to the class of lattice gas models (for a review see [1]) with near neighbour exclusion, e.g. dimers [2], hard-squares [3], hard-hexagons [4] etc. The quantum version of the model was introduced in [5] and studied by exact diagonalization and finite-size scaling, later the classical version was investigated by

† Permanent address: Central Research Institute for Physics, H-1525 Budapest, Hungary.

Monte Carlo (MC) simulations [6]. Although results for dimers ($m = 2$) were clearly in favour of Ising-like critical behaviour, for larger rods $m \geq 3$ no definite answer could be obtained from the numerical results. Evidently the sizes of systems used in the calculations (33 for finite-size scaling and 60×60 for MC) were not large enough to reach the asymptotic region of the critical point.

In the present paper—in order to clarify the properties of the transition for $m = 3$ and $m = 4$ —we extend the previous MC simulations [6] using larger systems with a rectangular shape elongated in the x direction. The largest systems we used were 512×128 and 1024×32 . The simulations were performed on the DISP (Delft Ising system processor) [7] which has a speed of over 10^6 spin updates s^{-1} . Hence the effective computational time has been increased by a factor of 10^3 in comparison with [6].

For simplicity, in the actual calculation we have chosen $K = K^y = K_1$ and used a histogramming method [8] to deduce the necessary thermodynamic information in the whole scaling regime from the results of a few simulations performed close to the critical point K_c . Furthermore we have determined the spin-spin correlation function in the x direction near to the critical point using a special purpose hardware correlator incorporated in the DISP. This correlator (built by J P L van Amen [9]) accumulates the product of spins along lines in the x direction of the lattice over all distances up to half the lattice size. This calculation is performed at intervals of a few sweeps (the DISP was instructed to visit spins randomly; one sweep is defined as the same number of spin update attempts as there are spins in the lattice) and is performed simultaneously with the MC process.

The structure of the paper is as follows. In section 2 some known results about chiral symmetry breaking—relevant to our models—are reviewed, together with the basic concepts of anisotropic scaling. Results of the simulations for the $m = 3$ and $m = 4$ models are presented in sections 3 and 4, respectively. Finally, a discussion about the character of the transitions of the two models can be found in section 5.

2. The chiral Potts model and anisotropic scaling

Although the ground state of the models defined earlier is m -fold degenerate, the permutation symmetry of the Potts model is not applicable. Labelling the ground states with positive spins at positions $x = x_+$ by an integer $k = x_+ \bmod m$, it is clear that the energy of a horizontal interface (parallel to the x direction) between different phases k_1 and k_2 does not depend on k_1 and k_2 . However, the energy of a vertical interface does. Such an interface corresponds with inserting $k_2 - k_1 + m \bmod m$ extra columns of negative spins, thus costing a proportional amount of energy when $K_1 > 0$.

The phase diagram associated with chiral symmetry breaking was investigated by Ostlund [10], and the critical scaling behaviour by den Nijs [11]. Although for $m = 3$ the chiral asymmetry is found to be relevant, they report no evidence that, at least for small asymmetry, the three-state Potts behaviour is modified. At stronger asymmetry a Lifshitz point is predicted [12–15], where the (three-state Potts) critical line splits in a Kosterlitz–Thouless [16] and a commensurate–incommensurate [17–19] transition line, with a floating phase in between. However, Haldane and others [20–22] find that the floating phase persists for all non-zero asymmetries. Ostlund predicts the latter scenario for the analogous four-state model [10].

The anisotropy of the chiral perturbation allows for the possibility of anisotropic scaling. Such scaling behaviour has indeed been reported at Lifshitz points and at commensurate-incommensurate transitions. Anisotropic scaling has been discussed in detail by Binder and Wang [23]; here we summarize only those aspects needed in our analysis. Anisotropic scaling may be formulated on the basis of a rescaling of the temperature field t by a factor u , resulting in different geometric scale factors in the x and y directions:

$$\begin{aligned}
 t &\rightarrow t' = ut \\
 x &\rightarrow x' = u^{-\nu_x} x \\
 y &\rightarrow y' = u^{-\nu_y} y \\
 f_s &\rightarrow f'_s = u^{\nu_x + \nu_y} f_s
 \end{aligned}
 \tag{2.1}$$

where f_s is the singular part of the reduced free energy per spin. Choosing $u = |t|^{-1}$ in the scaling relation of f_s and differentiating twice with respect to t shows that the bulk specific heat diverges with an exponent

$$\alpha = 2 - \nu_x - \nu_y
 \tag{2.2}$$

when $t \rightarrow 0$.

Since correlation lengths in the x and y directions scale as x and y , the divergences at the critical point have exponents ν_x and ν_y , respectively. The scaling of the magnetic field h requires another exponent denoted w :

$$h \rightarrow h' = u^w h.
 \tag{2.3}$$

Differentiating the scaling relation for the free energy twice with respect to h and taking $h = 0$ then similarly shows that the divergence of the susceptibility χ when $|t| \rightarrow 0$ is described by an exponent

$$\gamma = 2w - \nu_x - \nu_y.
 \tag{2.4}$$

The analysis of finite-size data with anisotropic scaling is subject to the complication that the rescaled system has a different shape. One way to solve this problem is to restrict the system sizes L_x in the x direction and L_y in the y direction to $L_x \gg L_y$. Including the finite sizes in the scaling relation of the free energy, differentiating twice to t and choosing $u = L_y^{1/\nu_y}$ yields

$$C(L_x, L_y) \sim L_y^{(2-\nu_x-\nu_y)/\nu_y} \sim L_y^{\alpha/\nu_y}
 \tag{2.5}$$

at $t = 0$, independent of L_x .

Differentiating instead to the magnetic field yields the finite-size dependence of the susceptibility

$$\chi(t = 0) \sim L_y^{\gamma/\nu_y}
 \tag{2.6}$$

Let the spin-spin correlation function $g(x, y, t)$ scale with a factor u^p . Writing the susceptibility as $\chi(t) = \int dx dy g(x, y, t)$ and rescaling the integral using $u = |t|^{-1}$, yields

$$\chi(t) \sim |t|^{p-\nu_x-\nu_y}
 \tag{2.7}$$

so that $p = \nu_x + \nu_y - \gamma$.

Another way to express p in other exponents is to choose $t = y = 0$ and $u = x^{1/\nu_x}$, or the same with x and y interchanged. This yields

$$p = \eta_x \nu_x = \eta_y \nu_y. \quad (2.8)$$

We will also consider the one-dimensional Fourier transform $G(q, L_y)$ of the correlation function in the x direction. We choose L_y so large that the correlation function (which is denoted $\tilde{g}(x, L_y)$ to express the dependence on the finite size L) becomes independent of L_x . Ignoring the oscillating behaviour of $\tilde{g}(x, L_y)$ that is expected for a lattice gas,

$$G(q, L_y) = \sum_{x=1}^{L_x} \tilde{g}(x, L_y) \exp(iqx). \quad (2.9)$$

Rescaling this formula using $u = L_y^{1/\nu_y}$, and replacing the sum by an integral, leads to

$$G(q = 0, L_y) \sim L_y^{\gamma/\nu_y - 1}. \quad (2.10)$$

This result for $q = 0$ generalizes simply to the wavenumber q_{\max} at the maximum of G when $\tilde{g}(x, L_y)$ oscillates. Determination of the structure factor G allows an analysis similar to that of the wavelength-dependent susceptibility such as that performed by Barber and Selke in the case of the ANNNI model [24].

3. Results for the $m = 3$ model

In the simulations we used periodic boundary conditions, and system sizes equal to powers of 2. These restrictions, which are imposed by the hardware of the DISP, are especially significant for the $m = 3$ model since the ground states of the model do not fit in the x direction. One expects alternation in the finite-size results, since even powers of 2 are equal to a multiple of 3 plus 1, whereas odd powers of 2 are equal to a multiple of 3 plus 2.

First, we present results on the specific heat. The approximate position of the maximum of the specific heat was located first, and then the actual energy distribution was determined from simulations close to this point. Then the position $K_{\max}(L)$ and the value $C_{\max}(L)$ of the specific heat maximum were obtained by the method described by Ferrenberg and Swendsen [8]. These values together with their statistical errors are presented in tables 1 and 2 for rectangular systems with sizes $4L \times L$ and $32L \times L$, respectively.

Table 1. Position and the value of the maximum of the specific heat for $m = 3$ models with size $4L \times L$. Finite-size estimates for α/ν_y calculated from equation (3.2) are presented in the last column.

$4L$	K_{\max}	C_{\max}	α/ν_y
16	0.4627(7)	0.393(3)	
32	0.4789(12)	0.568(5)	
64	0.5030(11)	0.957(26)	0.642(28)
128	0.5040(18)	1.275(21)	0.584(13)
256	0.5125(12)	1.798(83)	0.456(38)
512	0.5138(7)	2.28(21)	0.419(66)

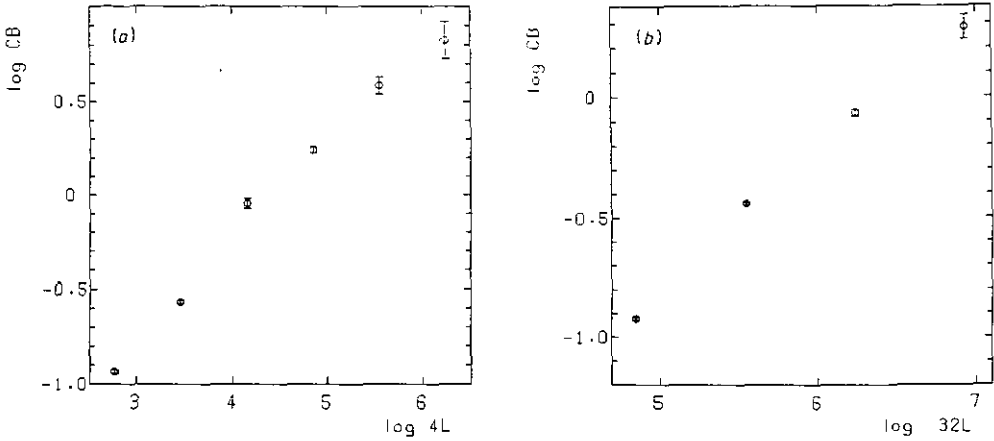


Figure 1. The maximum of the specific heat of the $m = 3$ model on rectangular finite lattices with sizes (a) $4L \times L$ and (b) $32L \times L$ versus the size of the system in the x direction on a log-log scale. Error bars appear only where they exceed the symbol size.

Table 2. Position and the value of the maximum of the specific heat for $m = 3$ models with size $32L \times L$. The estimates for α/ν_y were calculated using two subsequent entries for C_{\max} .

$32L$	K_{\max}	C_{\max}	α/ν_y
128	0.482(18)	0.398(2)	
256	0.492(10)	0.644(4)	0.69(1)
512	0.504(4)	0.937(13)	0.54(2)
1024	0.510(10)	1.331(65)	0.51(7)

The finite-size dependence of the numerical data for $K_{\max}(L)$ became small for the largest systems; thus the critical point of the model K_c can be estimated with the use of a $1/L$ correction term as

$$K_c = 0.516(3). \tag{3.1}$$

We expect that the maximum of the specific heat will obey equation (2.5); this relation is shown in figures 1(a) and (b) on a logarithmic scale for systems with shapes $4L \times L$ and $32L \times L$, respectively. To obtain a quantitative estimate for α/ν_y one has to take into account the alternation due to lattice sizes being equal to odd or even powers of 2. Thus we took pairs of values $C_{\max}(L)$ and $C_{\max}(4L)$ to estimate the critical exponent as

$$\frac{\alpha}{\nu_y}(4L) = \frac{\log(C_{\max}(4L)/C_{\max}(L))}{\log(4)}. \tag{3.2}$$

From these results, which are included in tables 1 and 2, one can observe that corrections to scaling are prominent for small L . We estimate

$$\frac{\alpha}{\nu_y} = 0.40 \pm 0.05 \tag{3.3}$$

The critical exponent of the magnetic susceptibility γ is determined using the scaling behaviour of the maximum of the structure factor at the critical point (equation (2.10)). We considered the ratio

$$R(L, K) = G_{\max}(L, K)/G_{\max}(L/2, K) \tag{3.4}$$

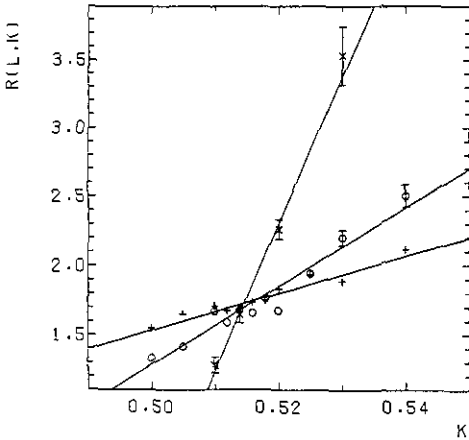


Figure 2. Ratio of the maxima of subsequent structure factors (equation (3.4)) for the $m = 3$ model on finite lattices with size $32L \times L$. The lines are a guide to the eye; the finite sizes are $L = 8$ (+), $L = 16$ (O) and $L = 32$ (x).

for systems of shape $32L \times L$. We note that for these elongated systems the effect of odd-even alternation is negligible. Furthermore the maximum of the structure factor was found at a wavevector slightly smaller than $2\pi/3$. We attribute the difference to the fact that the system sizes L_x are not a multiple of 3, and to incomplete ordering. $R(L, K)$ is plotted for $L = 8, 16$ and 32 in figure 2 for several values

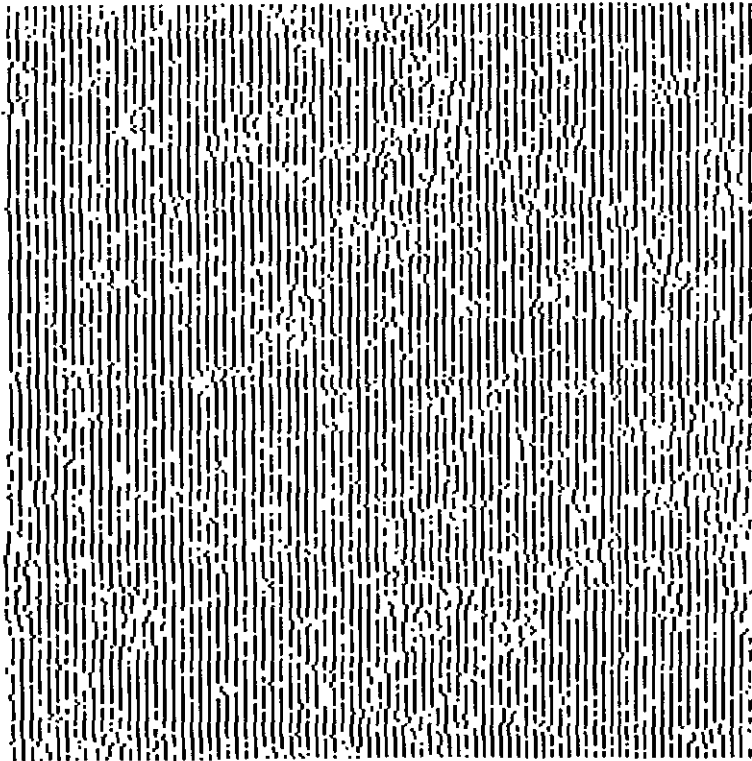


Figure 3. Spin configuration of a 256×256 $m = 3$ model at the phase transition ($K = 0.516$). Plus spins are black, minus spins are white. Locally, the system is already close to the ground state with a period of two white and one black columns. Domain walls appear as a shift in the positions of the columns.

of the coupling near the critical point. From the position of the crossing points of the $R(L, K)$ curves one can estimate the critical coupling as $K_c = 0.515(3)$, which coincides with the result from the specific heat analysis (equation (3.3)). From the value of the ratio at the critical point $R(L, K_c) = 2^{\gamma/\nu_y - 1}$ one gets an estimate for the critical exponent ratio

$$\gamma/\nu_y = 1.77 \pm 0.06. \tag{3.5}$$

A single intersection point such as that visible in figure 2, instead of a range where the curves coincide, implies an ordinary critical point instead of an incommensurate phase. As an illustration of the critical state of the $m = 3$ model, figure 3 shows the 256×256 spin configuration resulting from a simulation at $K = 0.516$. Further analysis of the data and a discussion about the possible universality class of the transition are postponed to section 5.

4. Results for the $m = 4$ model

The ordered ground state of the $m = 4$ model properly fits the system size to which simulations on the DISP are restricted, so that even-odd alternation of the results may be absent. In the same way as that described for the $m = 3$ model we determined the position and the value of the maximum of the specific heat for finite rectangular systems with sizes $4L \times L$ and $32L \times L$. The results are collected in tables 3 and 4, respectively, while the maximum of the specific heat is shown in figures 4(a) and (b) as a function of the system size for the two different aspect ratios, using a logarithmic scale. Finite-size extrapolants for the exponent α/ν_y are included in tables 3 and 4. These values were calculated in analogy to equation (3.2), but for the $m = 4$ model results on systems with linear sizes $2L$ and L were compared.

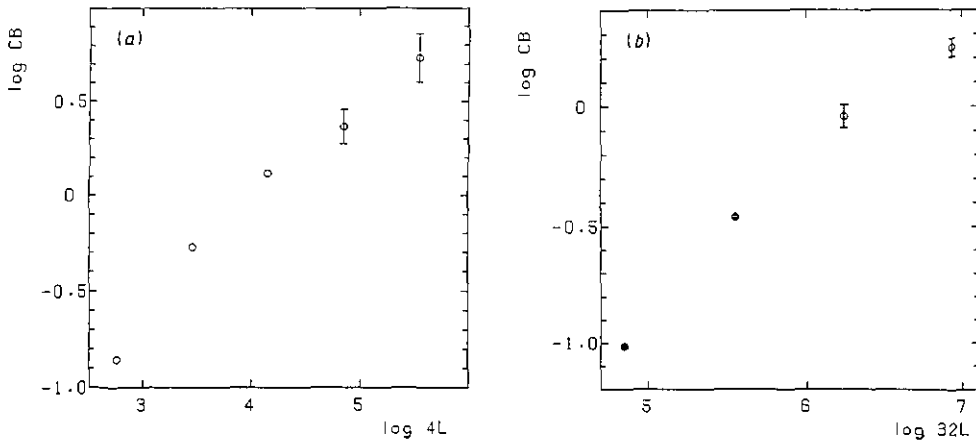


Figure 4. The maximum of the specific heat against system size L for rectangular $m = 4$ models for (a) $4L \times L$ and (b) $32L \times L$, on a log-log scale.

Extrapolating the finite-size data yields the following estimates:

$$K_c = 0.565 \pm 0.006 \tag{4.1}$$

Table 3. Position and the value of the maximum of the specific heat and estimates for α/ν_y for the $m = 4$ model calculated for $4L \times L$ systems.

$4L$	K_{\max}	C_{\max}	α/ν_y
16	0.4947(14)	0.426(6)	
32	0.5410(10)	0.762(4)	0.84(2)
64	0.5606(3)	1.123(14)	0.56(2)
128	0.5682(18)	1.44(13)	0.36(16)
256	0.5605(66)	2.08(27)	0.53(2)

Table 4. Position and the value of the maximum of the specific heat and estimates for α/ν_y for the $m = 4$ model calculated for $32L \times L$ systems.

$32L$	K_{\max}	C_{\max}	α/ν_y
128	0.500(10)	0.363(2)	
256	0.528(2)	0.632(4)	0.80(1)
512	0.541(1)	0.943(65)	0.58(10)
1024	0.551(2)	1.389(37)	0.56(11)

and

$$\alpha/\nu_y = 0.53 \pm 0.04. \quad (4.2)$$

We find that the energy distribution of the $m = 4$ system has two peaks, when the coupling constant is close to the value at the specific heat maximum for square and rectangular $4L \times L$ systems. The separation of the peaks shrinks to zero for large L . For square systems the peaks have approximately equal heights at the specific heat maximum, whereas for $4L \times L$ systems the peak at the lower energy is higher except for the 512×128 system. We observed two maxima for the specific heat in the 512×128 and 256×64 systems. The peak at the smaller coupling is the absolute maximum for the 256×64 system, while the other maximum is higher for the 512×128 system. The anomalous behaviour of these results may be related to the fact that the system is still finite in the x direction (see discussion).

The susceptibility exponent—as for the $m = 3$ model—is obtained from the ratio of the structure factors $R(L, K)$ (equation (3.4)) for $32L \times L$ systems. This ratio is plotted in figure 5 for $L = 8, 16$ and 32 , as a function of the coupling. As before, one may estimate the transition point from the crossing points of the curves: $K_c = 0.565(7)$ and the susceptibility exponent $\gamma/\nu_y = 1.65 \pm 0.2$. These results are slightly less accurate than those obtained from the analysis of the specific heat.

Next, we study the correlation function of the system near to the critical point. We computed the spin-spin correlation function $\bar{g}_L(K)$ in the y direction of square $L \times L$ systems over a distance $L/2$. The ratio

$$r(L, K) = \bar{g}_{2L}(K)/\bar{g}_L(K) \quad (4.3)$$

is shown in figure 6 for some values of K near the critical point. For large L the ratio $r(L, K)$ approaches 0 and 1 for $K < K_c$ and $K > K_c$, respectively, while at the critical point it is expected to satisfy the scaling relation $\lim_{L \rightarrow \infty} r(L, K_c) = 2^{-\eta_\nu}$. One can see from figure 6 that the transition takes place very close to the $r(L, K) = 1$ line, thus $\eta_\nu = 0.0 \pm 0.05$. The resulting estimate of the critical point is consistent with the previous ones: $K_c = 0.565(5)$.

Finally figure 7 illustrates the criticality of the $m = 4$ model. This configuration of 256×256 spins was obtained from a simulation at $K = 0.565$.

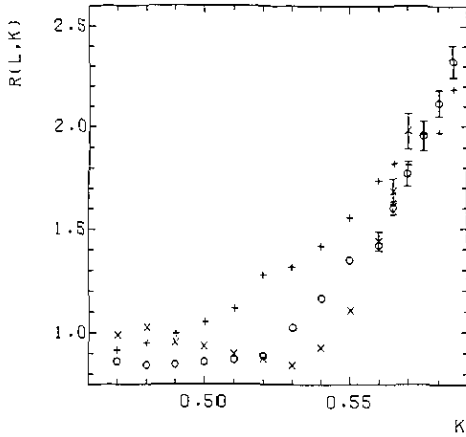


Figure 5. Ratio of the maxima of structure factors according to equation (3.4) for the $m = 4$ model for systems of size $32L \times L$. The finite sizes are $L = 8$ (+), $L = 16$ (O) and $L = 32$ (x).

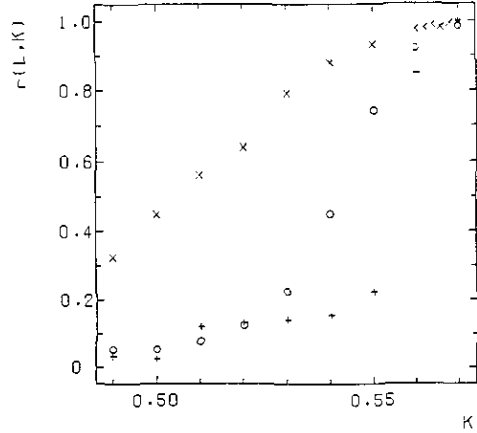


Figure 6. Ratio of spin-spin correlation functions over a distance of half the system size according to equation (4.3) for the $m = 4$ model on square lattices. The finite sizes are $L = 16$ (x) $L = 32$ (O) and $L = 64$ (+).

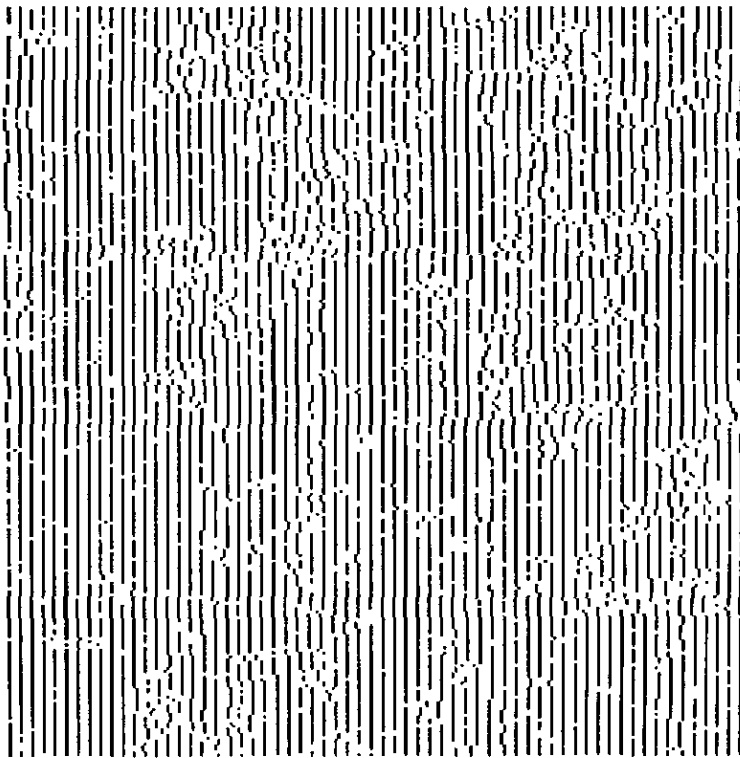


Figure 7. Spin configuration of a 256×256 $m = 4$ model at the phase transition ($K = 0.565$). Plus spins are black, minus spins are white. The ground state has a period of one black and three white columns. In this configuration, the periodicity has a tendency to be slightly larger than 4 (corresponding with altogether 63 black columns instead of 64), in agreement with a commensurate-incommensurate transition.

5. Possible universality class of the models

In previous studies [5, 6] no clear evidence was found about the type of the phase transition for the $m = 3$ and $m = 4$ models. The numerical results were interpreted slightly in favour of a first-order transition for both systems. However, the present, extended simulations show clear evidence that the transitions of both models are *second order*.

Numerical estimates of the critical exponents for the $m = 3$ model (equations (3.3) and (3.5)) are consistent with a transition of the three-state Potts type, thus characterized by the exponents [25]: $\nu_x = \nu_y = 5/6$, $\alpha/\nu = 2/5$ and $\gamma/\nu = 26/15 = 1.733$.

This identification is supported by the following approximate mapping of the $m = 3$ model on the three-state chiral Potts model. Following Huse and Fisher [26] we consider domains of the system characterized by their ground state $k_i = 0, 1, 2$ (see section 2). As was noted in section 2 the interaction energy per spin between two domains $\epsilon(k_1, k_2)$ is anisotropic. In the y direction it is the same as for the three-state Potts model $\epsilon_y(k_1, k_2) \sim \cos((2\pi/3)(k_1 - k_2))$, whereas in the x direction there is a chiral asymmetry: $\epsilon_x(k_1, k_2) \sim \cos((2\pi/3)(k_1 - k_2 + \Delta))$, with $\Delta = 1/4$. According to numerical studies [12–15] the transition of the three-state chiral Potts model at $\Delta = 1/4$ is probably the same as for $\Delta = 0$, i.e. it belongs to the universality class of the three-state Potts model. On the basis of this mapping (which stays valid also for $K_1 \neq K_y$) one may expect the same conclusion for the $m = 3$ model as well.

Identification of the universality class of the transition of the $m = 4$ model is more difficult. First we note that the exponent ratio (1.2) is inconsistent with a first-order transition which has $\alpha/\nu = 2.0$. Moreover, the scaling behaviour of the peak distance in the energy distribution leads to the same conclusion. The symmetry of the model allows for the presence of a cubic perturbation besides a chiral term in the effective Hamiltonian. These two perturbations have been studied separately [11, 27], however there is no result available about their simultaneous effect.

As far as the numerical results for the critical exponents are concerned, they are in agreement with a commensurate–incommensurate transition as first found by Kasteleyn [17], and also described by Pokrovsky and Talapov [18]. A recent review is given by Nagle *et al* [19]. The exponents are $\nu_x = 1/2$, $\nu_y = 1$, $\alpha/\nu_y = 1/2$, $\gamma/\nu_y = 3/2$ and $p = 0$.

At this point, however, we have to make three remarks. First, we could not obtain a reliable estimate for ν_x , since the size of the system in the x direction satisfying $L_x \leq L_y$ is too small. Thus we have no *direct* evidence for the presence of anisotropic scaling in our system. Our second remark concerns the floating phase, which is expected above the temperature of the Kasteleyn transition. We found no numerical evidence for the presence of such a floating phase (see figure 5). A possible explanation is that the floating phase is too narrow to be detected in the finite systems we used; however, we cannot exclude scenarios without a floating phase for our model. The third remark concerns a possible connection of the phase transition in the $m = 4$ model and that in the $N = 4$ state ‘superintegrable’ recently solved chiral Potts model [28, 29]. In this model the known thermal exponents (α , ν_x and ν_y) coincide with those at the Kasteleyn transition, however the magnetic exponents, i.e. γ , are not yet known for the former model.

In summary, our results indicate that the phase transitions in the $m = 3$ and 4 hard-rod models are continuous. For the $m = 3$ model, our numerical results and

an approximate mapping give clear evidence for a phase transition in the three-state Potts universality class. However the transition of the $m = 4$ model is probably anisotropic. Numerical estimates of the critical exponents agree with a Kasteleyn-type transition (and with the $N = 4$ superintegrable chiral Potts model); however, there is no evidence for a floating phase.

Acknowledgments

FI is indebted to the Laboratoire du Physique du Solide for hospitality in Nancy. The authors are indebted to F Mallezie for cooperation in the early stages of the work and to A Compagner for useful discussions. This research was supported in part by the Nederlandse Organisatie voor Wetenschappelijk Onderzoek (NWO) via the Stichting voor Fundamenteel Onderzoek der Materie (FOM).

References

- [1] Runnels L K 1972 *Phase Transitions and Critical Phenomena* vol 2, ed C Domb and M S Green (London: Academic) p 305
- [2] Fisher M E 1961 *Phys. Rev.* **124** 1664
Kasteleyn P W 1961 *Physica* **27** 1209
- [3] Huse D A 1982 *Phys. Rev. Lett.* **49** 1121
Baxter R J and Pearce P A 1983 *J. Phys. A: Math. Gen.* **16** 2239
- [4] Baxter R J 1980 *J. Phys. A: Math. Gen.* **13** L61
- [5] Iglói F 1989 *Phys. Rev. B* **40** 2362, 5187
- [6] Mallezie F 1990 *Phys. Rev. B* **41** 4475
- [7] Hoogland A, Spaa J, Selman B and Compagner A 1983 *J. Comput. Phys.* **51** 250
- [8] Ferrenberg A M and Swendsen R H 1988 *Phys. Rev. Lett.* **61** 2635
- [9] van Amen J P L 1988 *Afsnudeerverslag* TU Delft, unpublished
- [10] Ostlund S 1981 *Phys. Rev. B* **24** 398
- [11] den Nijs M P M 1984 *J. Phys. A: Math. Gen.* **17** L295
- [12] Selke W and Yeomans J 1982 *Z. Phys. B* **46** 311
- [13] Howes S F 1983 *Phys. Rev. B* **27** 1762
- [14] Duxbury P M, Yeomans J and Beale P D 1984 *J. Phys. A: Math. Gen.* **17** L179
- [15] Houlrik J M and Knak Jensen S J 1986 *Phys. Rev. B* **34** 325
- [16] Kosterlitz J M and Thouless D J 1973 *J. Phys. C: Solid State Phys.* **6** 1181
- [17] Kasteleyn P W 1963 *J. Math. Phys.* **A** **287**
- [18] Pokrovsky V L and Talapov A L 1979 *Phys. Rev. Lett.* **42** 65
- [19] Nagle J F, Yokoi S O and Bhattacharjee S M 1989 *Phase Transitions and Critical Phenomena* vol 13, ed C Domb and J L Lebowitz (London: Academic) p 235
- [20] Haldane F D M, Bak P and Bohr T 1983 *Phys. Rev. B* **28** 2743
- [21] Schulz H J 1980 *Phys. Rev. B* **22** 5274
- [22] von Gehlen G and Rittenberg V 1984 *Nucl. Phys. B* **230** 455
- [23] Binde K and Wang L S 1989 *J. Stat. Phys.* **55** 87
- [24] Barber M N and Selke W 1982 *J. Phys. A: Math. Gen.* **15** L617
- [25] den Nijs M P M 1979 *J. Phys. A: Math. Gen.* **12** 1857
- [26] Huse D A and Fisher M E 1982 *Phys. Rev. Lett.* **49** 793
- [27] Kadanoff L P and Brown A C 1979 *Ann. Phys., NY* **121** 318
- [28] Au-Yang H, McCoy B M, Perk J H H, Tang S and Yan M-L 1987 *Phys. Lett.* **123A** 219
- [29] Baxter R J 1989 *J. Stat. Phys.* **57** 1